

Atomic Layer Deposition Growth Reactions of  $\text{Al}_2\text{O}_3$  on  $\text{Si}(100)\text{-}2\times 1$ 

Mathew D. Halls and Krishnan Raghavachari\*

Department of Chemistry, Indiana University, Bloomington, Indiana 47405

Received: December 11, 2003; In Final Form: January 23, 2004

Cluster calculations employing hybrid density functional theory have been carried out to examine the atomistic details and thermochemistry of the early stages of  $\text{Al}_2\text{O}_3$  atomic layer deposition (ALD) on the  $\text{Si}(100)\text{-}2\times 1$  surface using the gas-phase precursors, trimethylaluminum (TMA) and  $\text{H}_2\text{O}$ . The critical point structures and enthalpies characterizing both the Al- and O-deposition half-reactions were investigated. Both sets of ALD half-reactions were found to be thermodynamically favorable and kinetically uninhibited. For all reactions the transition states and reaction products were determined to be lower in energy than the starting reactants. The  $\text{H}_2\text{O}$  ALD half-reactions were found to have an overall reaction enthalpy between  $-1.45$  and  $-1.63$  eV, with a transition state energy of  $-0.13$  to  $-0.21$  eV. The TMA ALD half-reactions were found to be exothermic by  $1.85\text{--}1.88$  eV. The transition state energy for the Al deposition half-reactions were determined to be  $-0.19$  to  $-0.27$  eV. Careful comparison of the reaction enthalpies suggests a small reactivity dependence on neighboring  $\text{-OH}^*$  groups, activating and suppressing the Al- and O-deposition ALD half-reactions, respectively.

## Introduction

Within a decade, semiconductor devices will require gate dielectric layers with thicknesses approaching 1 nm, which corresponds to only a few  $\text{SiO}_2$  atomic layers. At these dimensions, the fundamental limitations of  $\text{SiO}_2$  will impede continued miniaturization due to significant tunneling leakage.<sup>1–3</sup> Thus, the search for replacement gate oxide materials susceptible to precise deposition techniques is a central concern to the microelectronics industry. The most promising alternative dielectric materials consist of high- $\kappa$  binary metal oxides. One candidate material under widespread investigation is  $\text{Al}_2\text{O}_3$  deposited by atomic layer deposition (ALD).  $\text{Al}_2\text{O}_3$  is quite attractive because it is thermodynamically stable in contact with silicon,<sup>4</sup> has a band gap of 9 eV, and has a dielectric constant ( $k_{\text{Al}_2\text{O}_3} = 9.8$ ) about 3 times that of  $\text{SiO}_2$  ( $k_{\text{SiO}_2} = 3.9$ ).  $\text{Al}_2\text{O}_3$  growth by ALD involves film deposition through the cycling of self-terminating surface reactions, providing highly uniform conformal films with thickness control at the atomic layer level.<sup>5</sup> Each half-reaction involves exposure of the substrate to a gas-phase precursor, resulting in a maximum growth rate of one monolayer per exposure. The most often used precursors for  $\text{Al}_2\text{O}_3$  growth are trimethylaluminum ( $\text{Al}(\text{CH}_3)_3$ , TMA) and  $\text{H}_2\text{O}$  as the aluminum and oxygen sources, respectively.

Aspects of the reaction mechanism and thermochemistry of  $\text{Al}_2\text{O}_3$  ALD growth have been the focus of both experimental and theoretical investigations. Yates et al.<sup>6</sup> used infrared (IR) spectroscopy to elucidate the reaction mechanism of TMA with oxide surfaces. TMA was found to react readily with surface  $\text{-OH}$  groups, depositing  $\text{-Al}(\text{CH}_3)_2$  on the surface and liberating  $\text{CH}_4$ . In the ALD process, subsequent treatment of the Al surface species with  $\text{H}_2\text{O}$  results in new surface  $\text{-OH}$  groups, again releasing  $\text{CH}_4$ . Widjaja and Musgrave studied some aspects of the ALD half-reactions for growth on a  $\text{Al}_2\text{O}_3$  substrate using quantum chemical methods, employing  $\text{Al}(\text{OH})_n\text{-(CH}_3)_m$  clusters to represent the  $\text{Al}_2\text{O}_3$  surface.<sup>7</sup> Recent work

by Chabal and co-workers has been directed toward spectroscopic studies examining the process and products of interface formation during ALD of  $\text{Al}_2\text{O}_3$  on silicon surfaces.<sup>8</sup> In our group, complementary efforts have been directed toward examining the energetics and atomistic details of chemical reaction paths for  $\text{Al}_2\text{O}_3$  growth on technologically relevant substrates. Previously, we have studied the initial surface reaction pathways for TMA,  $\text{H}_2\text{O}$ , and the precursor side-reaction product dimethylaluminum hydroxide ( $\text{Al}(\text{CH}_3)_2\text{OH}$ , DMAOH) interacting with the  $2\times 1$  reconstructed hydrogen-terminated  $\text{Si}(100)$  surface.<sup>9,10</sup> In our work, the dominant surface reactions were found to be those with direct implication in  $\text{Al}_2\text{O}_3$  ALD growth mechanism,<sup>9</sup> leading to the formation of  $\text{Si-Al}$  and  $\text{Si-O}$  surface linkages, and a unique reaction pathway was identified for DMAOH leading to the deposition of  $\text{-O-Al}(\text{CH}_3)_2$  on the surface.<sup>10</sup>

In the present work, we shift our research efforts from the initial  $\text{Al}_2\text{O}_3$  ALD surface reactions<sup>9,10</sup> to the subsequent growth reaction pathways on the  $2\times 1$  reconstructed  $\text{Si}(100)$  surface. First-principles calculations based on hybrid density functional theory are carried out on a silicon cluster model to investigate the reaction enthalpies and atomistic details of the TMA and  $\text{H}_2\text{O}$  half-reactions for ALD growth on the  $\text{Si}(100)\text{-}2\times 1$  surface. The activation energies and enthalpies for the growth reactions on the surface of up to two  $\text{-O-Al}$  layers are calculated, corresponding to three  $\text{Al}_2\text{O}_3$  ALD half-reaction exposures.

## Computational Details and Surface Models

The calculations presented in this work were carried out using the Gaussian 03 suite of electronic structure programs.<sup>11</sup> All results described here are obtained using the B3-LYP hybrid functional, which corresponds to Becke's three parameter exchange functional (B3) along with the Lee-Yang-Parr gradient-corrected correlation functional (LYP).<sup>12,13</sup> To model the surface reaction site, a  $\text{Si}_9\text{H}_{12}$  cluster is used as employed in previous studies of the chemical reactivity and vibrational properties of the  $\text{Si}(100)\text{-}2\times 1$  surface.<sup>9,10,14–18</sup> The  $\text{Si}_9$  cluster

\* Corresponding author. E-mail: kraghava@indiana.edu.

corresponds roughly to one unit cell of the Si(100) surface. This cluster closely reproduces the local structure around the surface reaction site and consists of the Si dimer of the surface reaction site, four second-layer Si atoms, two third-layer Si atoms, and one fourth-layer Si atom. The cluster is terminated by hydrogen atoms to satisfy the valency of the cleaved Si–Si bonds during excision from the extended surface, giving a cluster stoichiometry of Si<sub>9</sub>H<sub>12</sub>. Boundary constraints, fixing atoms to their bulk tetrahedral positions, are imposed on the third- and fourth-layer silicons to avoid unphysical structural relaxation.<sup>19</sup> A multilevel basis set is employed in this work, denoted here as dzd<sub>2</sub>p, representing the first- and second-layer cluster atoms as well as the TMA and H<sub>2</sub>O atoms with the 6-31G\*\* basis set and the lower layer frozen cluster atoms with the 6-31G basis set.<sup>20,21</sup> Subject to the Si cluster boundary constraints, minimum energy structures were calculated for the reactants, transition structures, and product species for the growth half-reactions of TMA and H<sub>2</sub>O with the H/Si(100) cluster model. The nature of the calculated structures was verified by subsequent harmonic frequency calculations, which also yielded zero point energy (ZPE) corrections. All enthalpies reported here include ZPE corrections.

## Results and Discussion

In atomic layer deposition (ALD) a thin solid film is deposited through the cycling of self-terminating surface reactions. Each exposure of the substrate to a gas-phase precursor results in, at most, a single monolayer of growth via a self-limiting reaction. Consequently, ALD allows the deposition of a material through highly uniform and conformal growth, with thickness control at the atomic layer level. ALD was initially reported by Suntola and co-workers<sup>22</sup> for the directed growth of ZnS films. Since then, ALD has been developed for a variety of semiconductor materials.<sup>23–25</sup> In the ALD of binary oxides, a complete growth cycle consists of two half-reaction exposures, first exposing the surface to an oxygen precursor followed by exposure to a metal precursor, separated by a purge period. For the deposition of Al<sub>2</sub>O<sub>3</sub>, using H<sub>2</sub>O as the oxygen source, trimethylaluminum [Al-(CH<sub>3</sub>)<sub>3</sub>, TMA] is often used as the aluminum precursor, due to its thermal stability, high vapor pressure (8.4 Torr), and exothermic reaction with H<sub>2</sub>O.

In the present work, the energetics and atomic details of the ALD of  $\text{Al}_2\text{O}_3$  growth reactions in the early stages of deposition on the  $\text{Si}(100)\text{-}2\times 1$  surface are investigated. Previously, we have studied the initial ALD surface reactions using hybrid density functional theory representing the surface reaction site using the minimal  $\text{Si}_9$  surface dimer and larger  $\text{Si}_{15}$  double surface dimer cluster models.<sup>9</sup> The reaction energetics for the initial reactions between TMA and  $\text{H}_2\text{O}$  and the hydrogen-terminated  $\text{Si}(100)$  surface were found to be relatively insensitive to the effect of using a larger cluster to represent the Si substrate, with the  $\text{Si}_9$  and  $\text{Si}_{15}$  enthalpies agreeing to within 0.04 eV. Here we adopt the single-dimer  $\text{Si}_9$  cluster as the reaction site model of the  $\text{Si}(100)\text{-}2\times 1$  surface, which is suitable for early stages of ALD growth where the steric interactions between the growing  $\text{Al}_2\text{O}_3$  fragment and the Si substrate are minimal. The starting point for this study is the singly hydroxylated  $\text{Si}(100)$  surface, which is the product of the lowest energy  $\text{H}_2\text{O}$  initial surface reaction studied previously, shown in Figure 1.<sup>9,14</sup> This surface structure corresponds to the activated H/Si surface produced by the first  $\text{H}_2\text{O}$ -surface half-reaction, depositing surface  $-\text{OH}$  groups and liberating  $\text{H}_2$ . In our prior work, reaction with the H/Si(100) surface and TMA was found to have a lower activation energy; however, the surface hydroxylation reaction

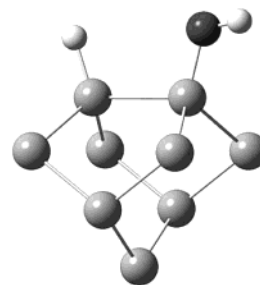
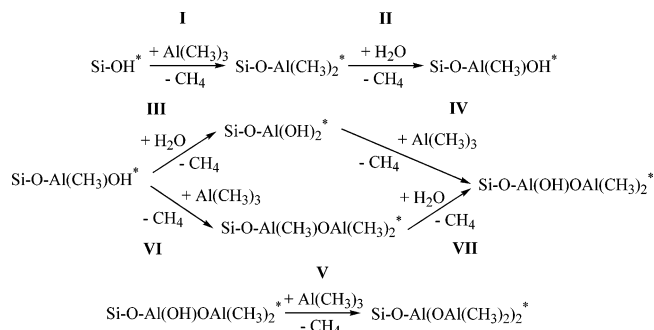
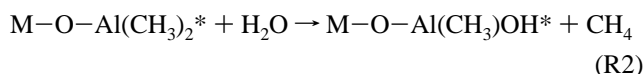
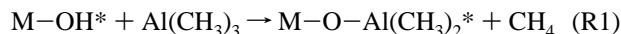


**Figure 1.** Structure of the  $\text{Si}_9\text{H}_{13}\text{OH}$  single-dimer cluster used to represent the reaction site on the  $\text{HO}/\text{Si}(100)\text{-}2\times 1$  surface in this work. (Terminal hydrogens omitted for clarity.)

**SCHEME 1**



with H<sub>2</sub>O was the enthalpically favored pathway by  $\sim 0.3$  eV.<sup>9</sup> At the B3-LYP/dzdp level of theory, the surface hydroxylation reaction between H<sub>2</sub>O and the H/Si surface was found to have an activation energy of 1.58 eV and to be energetically favorable, being exothermic overall by 0.69 eV. Subsequent alternating exposures of the HO/Si surface species to TMA and H<sub>2</sub>O result in the growth of Al<sub>2</sub>O<sub>3</sub>. The TMA and H<sub>2</sub>O half-reactions resulting in Al–O linkages can be denoted as

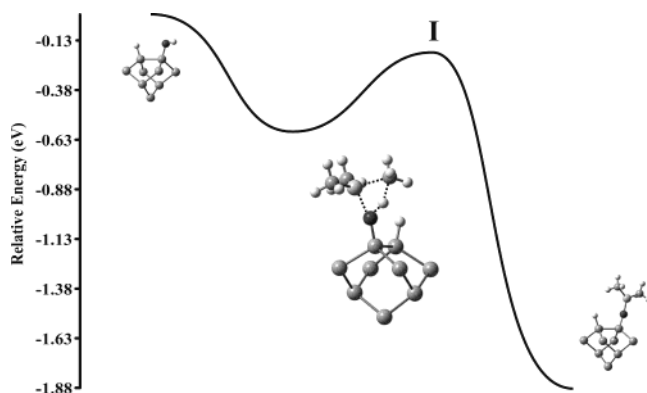


where M = Si for the initial reactions, M = Al for subsequent reactions, and the asterisks denote surface species. The reaction sequence explored in the current study is presented in Scheme 1, showing a total of seven half-reactions, denoted I through VII. Reactions I, IV, V, and VI are R1 half-reactions, corresponding to reaction of surface hydroxyls with the TMA precursor, and reactions II, III, and VII are R2 half-reactions, in which H<sub>2</sub>O reacts with the surface aluminum liberating CH<sub>4</sub>. In this work, reactions I through VII are separated into four groups for the purposes of discussion: I, II & III, IV & V, and VI & VII.

**Reactant Complexes.** As TMA approaches the HO/Si reaction site, it forms a reactant like TMA–surface complex, owing to interaction between the oxygen lone pairs and the empty p orbital of the aluminum atom. The Si–OH $\cdots$ TMA surface complex is bound by 0.59 eV, which can be compared to the gas-phase H<sub>2</sub>O $\cdots$ TMA complex which is predicted to be 0.72 eV more stable than the separated precursors.<sup>10</sup> In work by Widjaja and Musgrave,<sup>7</sup> the binding energy between TMA and a Al[OAl(OH)<sub>2</sub>]<sub>2</sub>OH cluster was computed to be 0.61 eV using B3-LYP/6-31+G\*\*. The TMA $\cdots$ HO/Si binding energy presented here is in good agreement. Similarly, as H<sub>2</sub>O impinges on the surface, specified by subsequent reaction products, it also forms a reactant–surface complex. For example, the Si–O–

**TABLE 1: Representative Bond Lengths for the Transition Structures and Activation Energies ( $E_a^\ddagger$ ) and Reaction Enthalpies ( $E^\circ$ ) for the  $\text{Al}_2\text{O}_3$  ALD Half-Reactions between TMA ( $\text{Al}(\text{CH}_3)_3$ ) and  $\text{H}_2\text{O}$  and the  $\text{H}/\text{Si}(100)$  Surface Calculated at the B3-LYP/dzdp Level of Theory**

reaction	TS structure	representative bond lengths ( $\text{\AA}$ )			$E_a^\ddagger$ (eV)	$E^\circ$ (eV)
		O–Al	O–H	Al–C		
$\text{Si}-\text{OH} + \text{Al}(\text{CH}_3)_3$	I	1.93	1.15	2.15	−0.19	−1.88
$\text{Si}-\text{O}-\text{Al}(\text{CH}_3)_2 + \text{H}_2\text{O}$	II	1.88	1.20	2.14	−0.21	−1.63
$\text{Si}-\text{O}-\text{Al}(\text{CH}_3)-\text{OH} + \text{H}_2\text{O}$	III	1.86	1.21	2.13	−0.16	−1.45
$\text{Si}-\text{O}-\text{Al}(\text{OH})_2 + \text{Al}(\text{CH}_3)_3$	IV	1.91	1.16	2.15	−0.25	−1.87
$\text{Si}-\text{O}-\text{Al}(\text{OH})-\text{O}-\text{Al}(\text{CH}_3)_2 + \text{Al}(\text{CH}_3)_3$	V	1.90	1.16	2.16	−0.27	−1.86
$\text{Si}-\text{O}-\text{Al}(\text{CH}_3)-\text{OH} + \text{Al}(\text{CH}_3)_3$	VI	1.90	1.17	2.16	−0.23	−1.85
$\text{Si}-\text{O}-\text{Al}(\text{CH}_3)-\text{O}-\text{Al}(\text{CH}_3)_2 + \text{H}_2\text{O}$	VII	1.87	1.21	2.13	−0.13	−1.48

**Figure 2.** Reaction energy profile for (I) the initial  $\text{Al}(\text{CH}_3)_3$  [TMA] Al-deposition ALD half-reaction on the  $\text{HO}/\text{Si}(100)$  surface calculated using the B3-LYP/dzdp level of theory. (Transition structures are shown, indicating transitional bonds by dashed lines.)

$\text{Al}(\text{CH}_3)_2 \cdots \text{H}_2\text{O}$  complex is found to be 0.86 eV lower in energy than the separated species. The corresponding binding energy with the  $\text{Al}[\text{OAl}(\text{OH})_2]_2\text{OH}$  cluster was found to be 0.74 eV.<sup>7</sup> For each half-reaction detailed here the reaction complex is bound by similar energies. Critical to note is that in every reaction described here the starting reactants are higher in energy than both the transition state and the final reaction product, and therefore the reactant complexes will not be discussed further.

**$\text{Al}_2\text{O}_3$  ALD TMA Half-Reaction I.** Reaction I corresponds to a R1 half-reaction in which TMA reacts with a surface hydroxyl group bonded directly to the underlying silicon substrate, involving the abstraction of the hydroxyl hydrogen by a TMA methyl group which is released as  $\text{CH}_4$ , depositing  $-\text{Al}(\text{CH}_3)_2$  on the surface. The reaction profile for reaction pathway I is shown in Figure 2, also showing the transition structure with dashed lines indicating partly broken/formed bonds. Representative bond lengths for the activated complex and relative enthalpies are presented in Table 1. From Figure 2 and the energies in Table 1, it can be seen that the initial TMA half-reaction is energetically favorable, having no activation energy and being significantly exothermic, overall. The transition state for reaction I is found to be 0.19 eV lower in energy than the separated reactants. Following the O–H and Al–C bonds throughout the course of the reaction shows values of 0.97 and 1.99  $\text{\AA}$  in the reactant complex, elongating to 1.15 and 2.15  $\text{\AA}$  in the transition structure, respectively, consistent with the ultimate breaking of these bonds. The O–Al bond length goes from 2.07  $\text{\AA}$  in the surface complex to 1.93  $\text{\AA}$  in the activated complex, and finally contracting to 1.72  $\text{\AA}$  in the  $\text{Si}-\text{O}-\text{Al}(\text{CH}_3)_2^*$  product, indicating complete bond formation. Overall, reaction I is found to be exothermic by 1.88 eV.

In this work, boundary conditions were applied to the terminal hydrogens and lowest layer silicon atoms, fixing them to their ideal tetrahedral lattice positions, to mimic the mechanical constraints on the surface site cluster model in the extended

$\text{Si}(100)-2 \times 1$  surface.<sup>19</sup> It is reasonable to expect that the effect of the boundary constraints on surface growth reaction energetics would be smaller than for other processes leading to changes in the native silicon lattice structure, such as Si–Si back-bond insertion. To estimate the influence of these geometric constraints on the reaction enthalpies reported here, calculations were carried out for the TMA half-reaction I relaxing the imposed constraints. Comparison of the fully relaxed and appropriately constrained results indicates that the effect is small. The fully relaxed activation energy and overall reaction enthalpy are within 0.02 eV of the constrained cluster results, being −0.19 and −1.90 eV, respectively at the B3-LYP/dzdp level of theory.

To estimate the possible deficiency of enthalpies calculated using the B3-LYP/dzdp level of theory due to an incomplete account of electron-correlation, coupled-cluster energy calculations including contributions from single, double, and perturbative triple excitations [CCSD(T)] were carried out on the B3-LYP/dzdp optimized critical-point structures for the TMA half-reaction I with the singly hydroxylated  $\text{H}/\text{Si}(100)$  surface. Comparison of the CCSD(T)/dzdp and B3-LYP/dzdp relative energies shows that the highly correlated energies favor the transition state and the product. The overall barrier is lowered by 0.13 eV, and the reaction becomes more exothermic by 0.15 eV. In light of this comparison, the barriers and overall enthalpies presented in this work may be more kinetically and thermodynamically favorable than indicated by the B3-LYP/dzdp results.

**$\text{Al}_2\text{O}_3$  ALD  $\text{H}_2\text{O}$  Half-Reactions II & III.** After the initial TMA exposure and following a purge period, O deposition through reaction with  $\text{H}_2\text{O}$  occurs next. Reactions II & III involve  $\text{H}_2\text{O}$  reacting with surface  $\text{Al}-\text{CH}_3$  species, in which a hydrogen atom from  $\text{H}_2\text{O}$  abstracts a surface methyl group, regenerating the surface  $-\text{OH}$  groups and again evolving  $\text{CH}_4$ . The surface reaction site in reaction II has two methyl groups:  $\text{Si}-\text{O}-\text{Al}(\text{CH}_3)_2^*$ . The energy surface for the  $\text{H}_2\text{O}$  half-reaction pathway II–III is shown in Figure 3, along with transition state structures with dashed lines indicating transitional bonds. As before, representative bond lengths for the activated complexes and relative enthalpies are presented in Table 1. Reaction II has a classical barrier height of −0.21 eV and is calculated to be 1.63 eV exothermic. The O–Al bond distance in the transition state for reaction II is 1.88  $\text{\AA}$  and becomes 1.71  $\text{\AA}$  in the  $\text{Si}-\text{O}-\text{Al}(\text{CH}_3)\text{OH}^*$  product. In R2 reaction III,  $\text{H}_2\text{O}$  reacts at the remaining  $\text{Al}-\text{CH}_3$  site, exchanging the methyl functional group with a hydroxyl, producing  $\text{Si}-\text{O}-\text{Al}(\text{OH})_2^*$ . The product for reaction III,  $\text{Si}-\text{O}-\text{Al}(\text{OH})_2^*$ , has an energy 1.45 eV lower than reactants. The O–Al and O–H bond distances in the product structure are 1.70 and 0.96  $\text{\AA}$ , which are 0.16 and 0.25  $\text{\AA}$  less than corresponding lengths in the transition structure. The transition state has an enthalpy of −0.16 eV. The enthalpies for reaction III can be compared with those for reaction II. The energetics of reaction III are slightly less



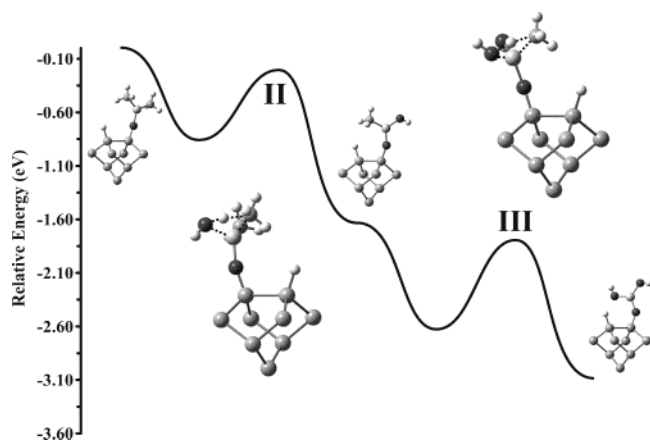


**Figure 3.** Reaction energy profile for the H<sub>2</sub>O O-deposition ALD half-reactions (II & II) with the growing Al<sub>2</sub>O<sub>3</sub> fragment on the Si(100) surface calculated using the B3-LYP/dzdp level of theory. (Transition structures are shown, indicating transitional bonds by dashed lines.)

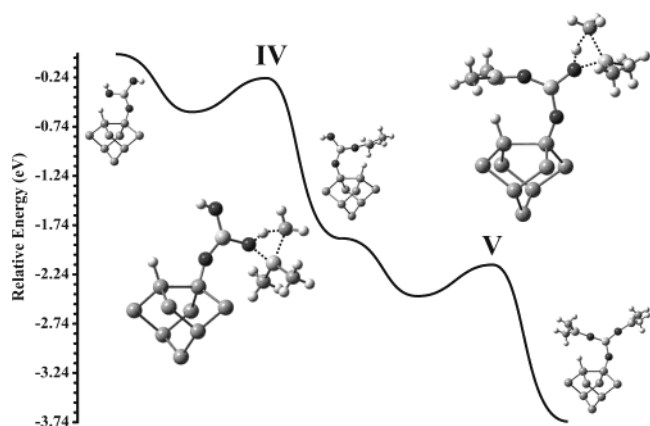


**Figure 4.** Reaction energy profile for the Al(CH<sub>3</sub>)<sub>3</sub> [TMA] Al-deposition ALD half-reactions (IV & V) with the growing Al<sub>2</sub>O<sub>3</sub> fragment on the Si(100) surface calculated using the B3-LYP/dzdp level of theory. (Transition structures are shown, indicating transitional bonds by dashed lines.)

favorable than those of reaction II by 0.05 and 0.18 eV for the barrier and reaction enthalpy, respectively. At the B3-LYP/dzdp level of theory, the H<sub>2</sub>O Al<sub>2</sub>O<sub>3</sub> ALD half-reaction pathway II–III is found to have no overall energy barrier and is highly exothermic by 3.08 eV.

**Al<sub>2</sub>O<sub>3</sub> ALD TMA Half-Reactions IV & V.** Surface reactions, IV & V, involve exposure of the growing Al<sub>2</sub>O<sub>3</sub>/Si substrate to the Al precursor, TMA. In these reactions, TMA reacts with one of the surface –OH\* groups, forming a new Al–O linkage (R1). The energy profile for reaction pathway IV–V is shown in Figure 4. Representative bond lengths for the activated complexes and relative enthalpies are presented in Table 1. Reaction IV results in the creation of –O–Al(OH)–OAl(CH<sub>3</sub>)<sub>2</sub>\* on the growing surface. The activation energy and reaction enthalpy for reaction IV are –0.25 and –1.87 eV, respectively. The transition state structure has O–Al and O–H bond lengths of 1.91 and 1.16 Å, which are elongated by ~0.2 Å with respect to the reactant structure. Further TMA exposure results in reaction at the second hydroxyl group (V). The transition state for the second TMA reaction is found to be 0.27 eV lower in energy than the reactants (0.02 eV less than TS IV). The transition state structure is shown in Figure 4 (V). At the activated complex the O–H and Al–C bonds are 1.16 and 2.16 Å. The O–Al bond length goes from 1.90 Å in the transition state to 1.72 Å in the Si–O–Al(OAl(CH<sub>3</sub>)<sub>2</sub>)<sub>2</sub>\*

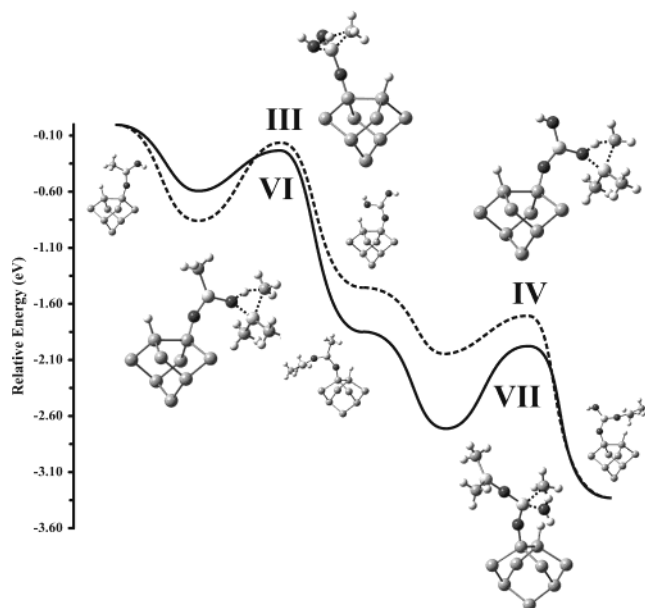


**Figure 5.** Reaction energy profile for the H<sub>2</sub>O/TMA ALD half-reactions (III & IV) with the growing Al<sub>2</sub>O<sub>3</sub> fragment on the Si(100) surface, along with a lower energy side-reaction pathway (VI & VII) due to an incomplete H<sub>2</sub>O half-reaction connecting the same reactant and product surface structures, calculated using the B3-LYP/dzdp level of theory. (Transition structures are shown, indicating transitional bonds by dashed lines.)

product, indicating complete bond formation. The reaction V surface product is calculated to be 1.86 eV lower in energy than reactants. Overall, the IV–V reactions have a reaction pathway enthalpy of –3.73 eV.

**Al<sub>2</sub>O<sub>3</sub> ALD Side-Reaction Pathways VI & VII.** The growth of Al<sub>2</sub>O<sub>3</sub> films using ALD typically requires a substrate incubation period following exposure to the Al- or O-deposition half-reaction precursor to ensure maximum monolayer growth. Full monolayer deposition can be difficult to achieve due to effects such as steric repulsions between adsorbates at adjacent reaction sites. To examine the reaction pathways available to the product of an incomplete H<sub>2</sub>O half-reaction, the stable intermediate of the II–III pathway, Si–O–Al(CH<sub>3</sub>)OH\*, is adopted as the starting reactant for the pathway consisting of reactions VI & VII. The reaction sequence VI–VII corresponds to a TMA half-reaction, R1, resulting in Si–O–Al(CH<sub>3</sub>)OAl(CH<sub>3</sub>)<sub>2</sub>\*, followed by a H<sub>2</sub>O half-reaction, R2. The reaction profile for the VI–VII pathway, along with reaction sequence III–IV, are shown in Figure 5; with transition state structures also shown. As before, representative bond lengths for the activated complexes and relative enthalpies are presented in Table 1. Reaction pathway VI–VII has two transition structures, one for each of the R1 and R2 ALD half-reactions. The R1 and R2 activation energies for VI and VII are calculated to be –0.23 and –0.13 eV, respectively. The geometric parameters for the activated complexes show only negligible differences from those obtained for the transition states for reactions III & IV (within 0.01 Å). The reaction enthalpies for reactions VI and VII are –1.85 and –1.48 eV. Comparison of the potential energy curves for the III–IV and VI–VII reaction pathways presented in Figure 5 indicates a notable difference. Composite reaction pathways III–IV and VI–VII start from the same reactants and end in the same products, and hence have the same overall reaction enthalpy of –3.33 eV; however, the order in which the R1/R2 half-reactions occur leads to changes in the relative energetics between the two pathways. The Al<sub>2</sub>O<sub>3</sub> side-reaction pathway (VI–VII) is the lower energy pathway, having transi-

tion states and intermediate product 0.07, 0.27, and 0.39 eV lower than the corresponding III–IV structures.

Using methods comparable to those employed here, Widjaja and Musgrave have previously studied the  $\text{Al}_2\text{O}_3$  ALD half-reactions R1 and R2 using  $\text{Al}(\text{OH})_n(\text{CH}_3)_m$  clusters to represent an  $\text{Al}_2\text{O}_3$  surface, which may be most representative of bulk  $\text{Al}_2\text{O}_3$  growth.<sup>7</sup> They found that the reaction enthalpies for the TMA and  $\text{H}_2\text{O}$  half-reactions were  $-1.70$  and  $-1.48$  eV, which are comparable to the results reported here. The activation energies, however, were much less favorable than the barriers calculated including an underlying Si substrate, being ca.  $-0.09$  and  $0.17$  eV, suggesting that the activation energies may be larger for bulk  $\text{Al}_2\text{O}_3$  growth. The results presented here outline the atomistic details and energetics for  $\text{Al}_2\text{O}_3$  ALD half-reactions on the Si(100) surface in the intermediate regime between the initial TMA/ $\text{H}_2\text{O}$  surface reactions<sup>9</sup> and the bulk  $\text{Al}_2\text{O}_3$  ALD growth process.

Comparison of the barrier heights for the R2  $\text{H}_2\text{O}$  half-reactions II and III suggests that the reactivity of the  $\text{Al}-\text{CH}_3^*$  group is slightly suppressed by the introduction of neighboring  $-\text{OH}^*$  groups, with the activation energy increasing by  $0.05-0.08$  eV with respect to reactions at a  $-\text{Al}(\text{CH}_3)_2$  reaction site. Conversely, a comparison of transition state energies for R1 TMA reactions I, IV, and V implies that the reactivity of the  $\text{Al}-\text{OH}^*$  group is very slightly enhanced by neighboring  $-\text{OH}^*$  groups. Similar changes in reactivity have been reported previously for the  $\text{Al}_2\text{O}_3$  ALD side-reaction product  $\text{Al}(\text{CH}_3)_2\text{-OH}$  (DMAOH).<sup>10</sup> Calculations involving larger clusters containing multiple silicon dimers should be performed in the future to consider the effects of steric interactions and to adequately treat a full monolayer of growth, including cross-linking reactions.

## Conclusions

The growth half-reactions between the  $\text{Al}_2\text{O}_3$  ALD precursors, TMA and  $\text{H}_2\text{O}$ , on the Si(100)- $2\times 1$  surface have been investigated using density functional cluster calculations. At the B3-LYP/dzdp level of theory, both the Al- and O-deposition half-reactions are thermodynamically and kinetically favored, being significantly exothermic and having no activation energy.

**Acknowledgment.** The authors gratefully acknowledge computational resources provided by the University Information Technology Services (UITs), Indiana University, and from NCSA (Grant No. CHE030049). M.D.H. also thanks the Department of Chemistry, Indiana University, for financial support provided by an Ernest R. Davidson Postdoctoral Fellowship.

## References and Notes

- (1) Wilk, G. D.; Wallace, R. M.; Anthony, J. M. *J. Appl. Phys.* **2001**, *89*, 5243.
- (2) Kingon, A. I.; Maria, J. P.; Streiffer, S. K. *Nature* **2000**, *406*, 1032.
- (3) Muller, D. A.; Sorsch, T.; Moccio, S.; Baumann, F. H.; Evans-Lutterodt, K.; Timp, G. *Nature* **1999**, *399*, 758.
- (4) Hubbard, K. J.; Schlom, D. G. *J. Mater. Res.* **1996**, *11*, 2757.
- (5) George, S. M.; Ott, A. W.; Klaus, J. W. *J. Phys. Chem.* **1996**, *100*, 13121.
- (6) Yates, D. J. C.; Dembinski, G. W.; Kroll, W. R.; Elliott, J. J. *J. Phys. Chem.* **1969**, *73*, 911.
- (7) Widjaja, Y.; Musgrave, C. B. *Appl. Phys. Lett.* **2002**, *80*, 3304.
- (8) Frank, M. M.; Chabal, Y. J.; Wilk, G. D. *Appl. Phys. Lett.* **2003**, *82*, 4758.
- (9) Halls, M. D.; Raghavachari, K. *J. Chem. Phys.* **2003**, *118*, 10221.
- (10) Halls, M. D.; Raghavachari, K.; Frank, M. M.; Chabal, Y. J. *Phys. Rev. B* **2003**, *68*, 161302R.
- (11) Frisch, M. J.; et al. *Gaussian 03*, Revision A.1; Gaussian, Inc.: Pittsburgh, PA, 2003.
- (12) Becke, A. D. *J. Chem. Phys.* **1993**, *98*, 5648.
- (13) Lee, C.; Yang, W.; Parr, R. G. *Phys. Rev. B* **1988**, *37*, 785.
- (14) Konecny, R.; Doren, D. J. *J. Chem. Phys.* **1997**, *106*, 2426.
- (15) Raghavachari, K.; Chabal, Y. J.; Struck, L. M. *Chem. Phys. Lett.* **1996**, *252*, 230.
- (16) Weldon, M. K.; Stefanov, B. B.; Raghavachari, K.; Chabal, Y. J. *Phys. Rev. Lett.* **1997**, *79*, 2851.
- (17) Struck, L. M.; Eng, J.; Bent, B. E.; Flynn, G. W.; Chabal, Y. J.; Christman, S. B.; Chabal, E. E.; Raghavachari, K.; Williams, G. P.; Rademacher, K.; Mantl, S. *Surf. Sci.* **1997**, *380*, 444.
- (18) Stefanov, B. B.; Gurevich, A. B.; Weldon, M. K.; Chabal, Y. J.; Raghavachari, K. *Phys. Rev. Lett.* **1998**, *81*, 3908.
- (19) Terminal hydrogens representing third or deeper layer silicons are held fixed at positions corresponding to a Si–H distance of  $1.48$  Å along ideal tetrahedral directions.
- (20) Hariharan, P. C.; Pople, J. A. *Theor. Chim. Acta* **1973**, *28*, 213.
- (21) Franci, M. M.; Petro, W. J.; Hehre, W. J.; Binkley, J. S.; Gordon, M. S.; DeFrees, D. J.; Pople, J. A. *J. Chem. Phys.* **1982**, *77*, 3654.
- (22) Pesa, M.; Makela, R.; Suntola, T. *Appl. Phys. Lett.* **1981**, *38*, 131.
- (23) Leskela, M.; Ritala, M. *Thin Solid Films* **2002**, *409*, 138.
- (24) Niinisto, L. *Curr. Opin. Solid State Mater. Sci.* **1998**, *3*, 147.
- (25) Ritala, M. *Appl. Surf. Sci.* **1997**, *112*, 223.